Lesion Characterization in Breast Imaging: VIPR-SSFP versus FSE

C. J. Moran[1], F. Kelcz[2], J. L. Klaers[1], Y. Jung[3], S. Fain[1,2], and W. F. Block[2,4]

[1]Medical Physics, University of Wisconsin, Madison, Wisconsin, United States, [2]Radiology, University of Wisconsin, Madison, Wisconsin, United States, [3]Electrical and Computer Engineering, University of Wisconsin, Madison, Wisconsin, United States, [4]Biomedical Engineering, University of Wisconsin, Madison, Wisconsin, United States

INTRODUCTION

Non-contrast-enhanced T2-weighted images are used clinically to improve the specificity of contrast-enhanced breast MRI. Signal intensity on T2-weighted images can clarify lesion characterization in cases of conflicting morphology and enhancement patterns [1]. However, standard T2-weighted Fast Spin Echo (FSE) sequences are limited by low through-plane resolution and long scan times required to acquire both fat-suppressed and non fat-suppressed datasets. In this work, we apply the 3D isotropic VIPR-SSFP method to breast imaging to provide T2-like image volumes, fat/water separation, and high isotropic resolution. The VIPR-SSFP image volumes with 0.63 mm isotropic resolution were compared to conventional 2D T2-weighted fat-suppressed FSE image volumes in five volunteers and three patients at 1.5T to determine how the highly increased morphologic detail of the VIPR-SSFP sequence improves the contribution of T2-weighted data to lesion characterization.

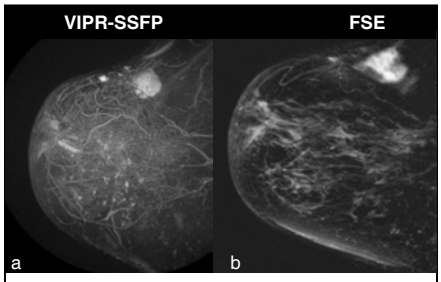

Figure 1. MIP of VIPR-SSFP water volume (a) and corresponding MIP of FSE data (b). In comparison to standard FSE images, VIPR-SSFP provides high structural detail due to high isotropic resolution and T2/T1 contrast.

MATERIALS AND METHODS

VIPR-SSFP [2] separates fat and water using the LC-SSFP (Linear Combination Steady State Free Precession) fat suppression technique [3]. While the optimal TR interval in LC-SSFP at 1.5T is quite short (2.4 ms), a dual-echo 3D radial acquisition (VIPR) allows for high spatial resolution within this TR constraint. An eight-coil breast array allows voxel volume to be reduced 50% (0.63x0.63x0.63 mm) with no increase in scan time relative to our earlier work with four coils (0.78x0.78x0.78 mm)[4]. LC–SSFP requires a center frequency at the mid-point between fat and water, and thus phase differences in each half-echo become more important with longer, higher resolution acquisitions. We now correct the phase of the desired signal component, which also provides additional dephasing for the unwanted component.

In earlier work we investigated VIPR-SSFP as a post contrast acquisition because of the high SNR and visibility of the vasculature [4]. However, the contrast agent obscured diagnostically significant morphologic characteristics. Therefore, non-contrast comparisons between FSE and the VIPR-SSFP sequence were obtained in five volunteer studies and three patient studies after obtaining informed consent according to the Institutional Review Board. Unilateral acquisitions using a sagittal excitation slab were acquired on a GE Signa 1.5T Echospeed scanner (GE Healthcare, Milwaukee, WI) using an 8 channel GE HD breast coil. The VIPR-SSFP scan acquired a 320 x 320 x 320 image matrix over a 20 cm FOV in five minutes (TR/TE/FA 2.9/0.4/30). The FSE acquisition acquired 0.62 x 0.62 x 4.0 mm slices in four minutes over a 16 cm FOV (TR/TE:2500/128).

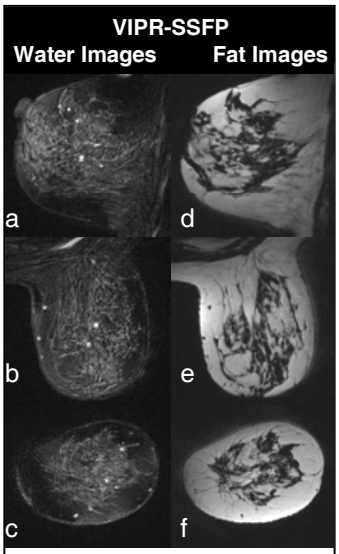

Figure 2. Sagittal (a,d), axial (b,e), and coronal (c,f) 2 mm slice reformats from both the water (a-c) and fat (d-f) VIPR-SSFP image volumes at 0.63 mm isotropic resolution. Three 0.63 mm slices are averaged in each plane to increase SNR.

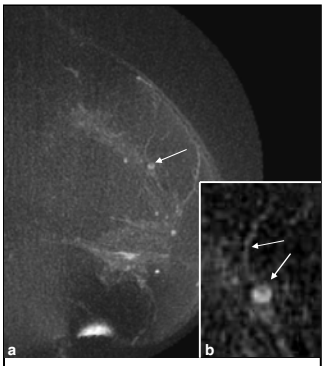

Figure 3. VIPR-SSFP image (a) shows a 3-4 mm diameter lymph node (white arrow) that is imperceptible on standard T2-weighted images. Fatty hilum and incoming vessel characteristic of lymph node are identifiable (b).

RESULTS AND DISCUSSION

VIPR-SSFP produces high isotropic resolution (0.63x0.63x0.63 mm) and T2-like contrast (Figure 1). While the total scan time for an FSE exam is 20% shorter than that required for a VIPR-SSFP acquisition, the FSE voxel volume is twice as large and FSE does not simultaneously provide both fat and water image volumes. Figure 2 shows the VIPR-SSFP fat and water images in sagittal, axial, and coronal reformats. The availability of both the fat and water volumes in VIPR-SSFP is important because the fat images can be used, for instance, to detect spiculation of low T2 malignancies against the fat. The main improvement over standard FSE imaging that the VIPR-SSFP technique provides is the reduction of through-plane partial volume effects. In Figure 3, a lymph node (white arrow) is identified by its fatty hilum and incoming vessel in the VIPR-SSFP method. This lymph node was not discernable on the FSE images. The probable lobulated cyst in Figure 4 also exemplifies the increased morphologic detail available with VIPR-SSFP. Ultimately, VIPR-SSFP allows the radiologist to make choices about the trade-off between partial voluming and SNR after the scan, rather than requiring this decision to be made at scan time.

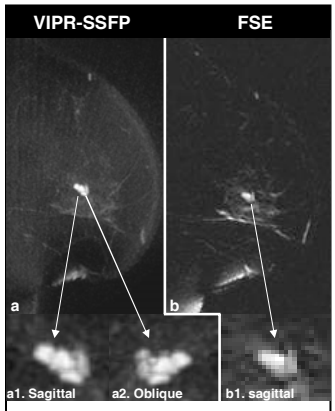

Figure 4. VIPR-SSFP image (a) of a lobulated non-enhancing mass (probably a mildly complex cyst) displays superb internal detail compared with the FSE scan (b). Magnified images of lobulated cyst with FSE (b1) and VIPR-SSFP sagittal (a1) and oblique (a2) reformat.

CONCLUSIONS

The volunteer and patient studies comparing VIPR-SSFP to conventional FSE demonstrate the T2-like contrast and increased morphologic detail available with the VIPR-SSFP method. The VIPR-SSFP technique alleviates the partial voluming limitations of FSE and provides water and fat image volumes in approximately the same amount of time required to acquire only a fat-suppressed FSE dataset. Specifically, the VIPR-SSFP sequence provides improved anatomic definition of small structures such as fatty hilum and entering vessels for lymph nodes and internal septations in fibroadenomas. Based on these results, we have begun a 25-patient study to gauge the effect of the VIPR-SSFP method on differential diagnosis in breast MRI.

Acknowledgements Research supported by NIH 5T32 CA09206-26 and NIH NCI 1R01CA116380-01A1. We also gratefully acknowledge the support of GE Healthcare.

References 1. Kuhl CK, *et al.*, JMRI, 9:187-196, 1999. 2. Lu AM, *et al.*, *MRM,* 53:692-699, 2005. 3. Vasanawala SS, *et al.*, MRM, 43:82-90, 2000 4.Moran C, *et al.*, Proc. 14th ISMRM, 2868, 2006.